

# MoleculeNet: A Benchmark for Molecular Machine Learning

Zhenqin Wu,<sup>†,||</sup> Bharath Ramsundar,<sup>‡,||</sup> Evan N. Feinberg,<sup>¶,⊥</sup> Joseph Gomes,<sup>†,⊥</sup>  
Caleb Geniesse,<sup>¶</sup> Aneesh S. Pappu,<sup>‡</sup> Karl Leswing,<sup>§</sup> and Vijay Pande<sup>\*,†</sup>

<sup>†</sup>*Department of Chemistry, Stanford University*

<sup>‡</sup>*Department of Computer Science, Stanford University*

<sup>¶</sup>*Program in Biophysics, Stanford School of Medicine*

<sup>§</sup>*Schrodinger Inc.*

<sup>||</sup>*Joint First Authorship*

<sup>⊥</sup>*Joint Second Authorship*

E-mail: pande@stanford.edu

## Abstract

Molecular machine learning has been maturing rapidly over the last few years. Improved methods and the presence of larger datasets have enabled machine learning algorithms to make increasingly accurate predictions about molecular properties. However, algorithmic progress has been limited due to the lack of a standard benchmark to compare the efficacy of proposed methods; most new algorithms are benchmarked on different datasets making it challenging to gauge the quality of proposed methods. This work introduces MoleculeNet, a large scale benchmark for molecular machine learning. MoleculeNet curates multiple public datasets, establishes metrics for evaluation, and offers high quality open-source implementations of multiple previously proposed molecular featurization and learning algorithms (released as part of the

DeepChem open source library). MoleculeNet benchmarks demonstrate that learnable representations, and in particular graph convolutional networks, are powerful tools for molecular machine learning and broadly offer the best performance. However, for quantum mechanical and biophysical datasets, the use of physics-aware featurizations can be significantly more important than choice of particular learning algorithm.

## Introduction

With the advent of sophisticated deep learning methods,<sup>1</sup> machine learning has gathered increasing amounts of attention from the scientific community. Over the past few years, data-driven analysis has become a routine step in many chemical and biological applications, including virtual screening,<sup>2-5</sup> chemical property prediction,<sup>6</sup> and quantum chemistry calculations.<sup>7,8</sup> In many such applications, machine learning has shown strong potential to compete with or even outperform conventional *ab-initio* computations.<sup>8,9</sup> It follows that introduction of novel machine learning methods has the potential to reshape research on properties of molecules. However, this potential has been limited by the lack of a standard evaluation platform for proposed machine learning algorithms. Algorithmic papers often benchmark proposed methods on disjoint dataset collections, making it a challenge to gauge whether a proposed technique does in fact improve performance.

Data for molecule-based machine learning tasks are highly heterogeneous and expensive to gather. Obtaining precise and accurate results for chemical properties typically requires specialized instruments as well as expert supervision (contrast with computer speech and vision, where lightly trained workers can annotate data suitable for machine learning systems). As a result, molecular datasets are usually much smaller than those available for other machine learning tasks. Furthermore, the breadth of chemical research means our interests with respect to a molecule may range from quantum characteristics to measured impacts on the human body. Molecular machine learning methods have to be capable of learning to predict this very broad range of properties. Complicating this challenge, input

molecules can have arbitrary size and components, highly variable connectivity and many three dimensional conformers (three dimensional molecular shapes). To transform molecules into a form suitable for conventional machine learning algorithms (that usually accept fixed length input), we have to extract useful and related information from a molecule into a fixed dimensional representation (a process called featurization).<sup>10-12</sup>

To put it simply, building machine learning models on molecules requires overcoming several key issues: limited amounts of data, wide ranges of outputs to predict, large heterogeneity in input molecular structures and appropriate learning algorithms. Therefore, this work aims to facilitate the development of molecular machine learning methods by curating a number of dataset collections, creating a suite of software that implements many known featurizations of molecules, and providing high quality implementations of many previously proposed algorithms. Following the footsteps of WordNet<sup>13</sup> and ImageNet,<sup>14</sup> we call our suite MoleculeNet, a benchmark collection for molecular machine learning.

In machine learning, a benchmark serves as more than a simple collection of data and methods. The introduction of the ImageNet benchmark in 2009 has triggered a series of breakthroughs in computer vision, and in particular has facilitated the rapid development of deep convolutional networks. The ILSVRC, an annual contest held by the ImageNet team,<sup>15</sup> draws considerable attention from the community, and greatly stimulates collaborations and competitions across the field. The contest has given rise to a series of prominent machine learning models such as AlexNet,<sup>16</sup> GoogLeNet,<sup>17</sup> ResNet<sup>18</sup> which have had broad impact on the academic and industrial computer science communities. We hope that MoleculeNet will trigger similar breakthroughs by serving as a platform for the wider community to develop and improve models for learning molecular properties.

In particular, MoleculeNet contains data on the properties of nearly 600,000 compounds. All datasets have been curated and integrated into the open source DeepChem package.<sup>19</sup> Users of DeepChem can easily load all MoleculeNet benchmark data through provided library calls. MoleculeNet also contributes high quality implementations of well known (bio)chemical

featurization methods. To facilitate comparison and development of new methods, we also provide high quality implementations of several previously proposed machine learning methods. Our implementations are integrated with DeepChem, and depend on Scikit-Learn<sup>20</sup> and Tensorflow<sup>21</sup> underneath the hood. Finally, evaluation of machine learning algorithms requires defined methods to split datasets into train/valid/test collections. Random splitting, common in machine learning, is often not correct for chemical data.<sup>22</sup> MoleculeNet contributes a library of splitting mechanisms to DeepChem and evaluates all algorithms with multiple choices of data split. MoleculeNet provide a series of benchmark results of implemented machine learning algorithms using various featurizations and splits upon our dataset collections. These results are provided within this paper, and will be maintained online in an ongoing fashion as part of DeepChem.

The related work section will review prior work in the chemistry community on gathering curated datasets and discuss how MoleculeNet differs from these previous efforts. The methods section reviews the dataset collections, metrics, featurization methods, and machine learning models included as part of MoleculeNet. The results section will analyze the benchmarking results to draw conclusions about the algorithms and datasets considered.

## Related Work

MoleculeNet draws upon a broader movement within the chemical community to gather large sources of curated data. PubChem<sup>23</sup> and PubChem BioAssay<sup>24</sup> gather together thousands of bioassay results, along with millions of unique molecules tested within these assays. The ChEMBL database offers a similar service, with millions of bioactivity outcomes across thousands of protein targets. Both PubChem and ChEMBL are human researcher oriented, with web portals that facilitate browsing of the available targets and compounds. ChemSpider is a repository of nearly 60 million chemical structures, with web based search capabilities for users. The Crystallography Open Database<sup>25</sup> and Cambridge Structural Database<sup>26</sup> offer

large repositories of organic and inorganic compounds. The protein data bank<sup>27</sup> offers a repository of experimentally resolved three dimensional protein structures. This listing is by no means comprehensive; the methods section will discuss a number of smaller data sources in greater detail.

These past efforts have been critical in enabling the growth of computational chemistry. However, these previous databases are not machine-learning focused. In particular, these collections don't define metrics which measure the effectiveness of algorithmic methods in understanding the data contained. Furthermore, there is no prescribed separation of the data into training/validation/test sets (critical for machine learning development). Without specified metrics or splits, the choice is left to individual researchers, and there are indeed many chemical machine learning papers which use subsets of these data stores for machine learning evaluation. Unfortunately, the choice of metric and subset varies widely between groups, so two methods papers using PubChem data may be entirely incomparable. MoleculeNet aims to bridge this gap by providing benchmark results for a reasonable range of metrics, splits, and subsets of these (and other) data collections.

It's important to note that there have been some efforts to create benchmarking datasets for machine learning in chemistry. The Quantum Machine group<sup>28</sup> and previous work on multitask learning<sup>3</sup> both introduce benchmarking collections which have been used in multiple papers. MoleculeNet incorporates data from both these efforts and significantly expands upon them.

## Methods

MoleculeNet is based on the open source package Deepchem.<sup>19</sup> Figure 1 shows an annotated DeepChem benchmark script. Note how different choices for data splitting, featurization, and model are available. In this section, we will further elaborate the benchmarking system, introducing available datasets as well as implemented splitting, featurization, and learning

methods.

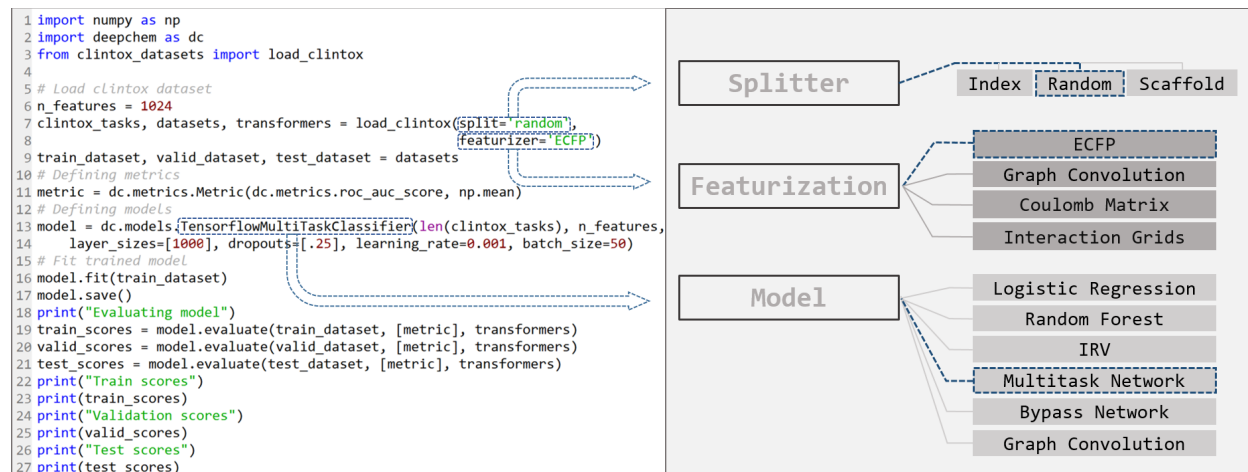


Figure 1: Example code for benchmark evaluation with DeepChem, multiple methods are provided for data splitting, featurization and learning.

## Datasets

MoleculeNet is built upon multiple public databases. The full collection currently includes over 600,000 compounds tested on a range of different properties. These properties can be subdivided into four categories: quantum mechanics, physical chemistry, biophysics and physiology. As illustrated in Figure 2 and Table 1, separate datasets in the MoleculeNet collection cover various levels of molecular properties, ranging from atomic-level properties to macroscopic influences on human body.

In most datasets, SMILES strings<sup>29</sup> are used to represent input molecules. Properties, or output labels, are either 0/1 for classification tasks, or floating point numbers for regression tasks. At the time of writing, MoleculeNet contains 12 datasets prepared and benchmarked, but we anticipate adding further datasets in an on-going fashion. The number of compounds and tasks for each dataset are listed in Table 1. Other details will be elaborated in this subsection.

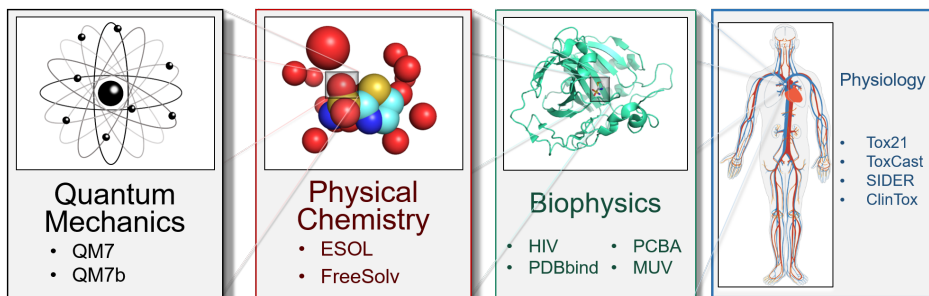


Figure 2: Tasks in different datasets focus on different levels of properties of molecules

Table 1: Dataset Details: number of compounds and tasks

| Category           | Dataset  | Description           | Tasks | Compounds |
|--------------------|----------|-----------------------|-------|-----------|
| Quantum Mechanics  | QM7      | atomization energy    | 1     | 7165      |
|                    | QM7b     | electronic properties | 14    | 7211      |
| Physical Chemistry | ESOL     | solubility            | 1     | 1128      |
|                    | FreeSolv | solvation energy      | 1     | 643       |
| Biophysics         | PCBA     | bioactivity           | 128   | 439863    |
|                    | MUV      | bioactivity           | 17    | 93127     |
|                    | PDBbind  | binding affinity      | 1     | 11908     |
|                    | HIV      | bioactivity           | 1     | 41913     |
| Physiology         | Tox21    | toxicity              | 12    | 8014      |
|                    | ToxCast  | toxicity              | 617   | 8615      |
|                    | SIDER    | side effect           | 27    | 1427      |
|                    | ClinTox  | clinical toxicity     | 2     | 1491      |

## QM7 and QM7b

The QM7/QM7b datasets are subsets of the GDB-13 database,<sup>30</sup> a database of nearly 1 billion stable and synthetically accessible organic molecules, containing up to seven “heavy” atoms (C, N, O, S). The 3D Cartesian coordinates of the most stable conformation and electronic properties (atomization energy, HOMO/LUMO eigenvalues, etc.) of each molecule were determined using *ab-initio* density functional theory (PBE0/tier2 basis set).<sup>7,8</sup> Learning methods benchmarked on QM7/QM7b are responsible for predicting these electronic properties given stable conformational coordinates.

Both of these datasets were processed as part of the Quantum-Machine effort,<sup>28</sup> which

has processed a number of datasets to measure the efficacy of machine-learning methods for quantum chemistry. This effort has additional datasets which are in the process of being integrated into the MoleculeNet suite.

## **ESOL**

ESOL is a small dataset consisting of water solubility data for 1128 compounds.<sup>6</sup> The dataset has been used to train models that estimate solubility directly from chemical structures (as encoded in SMILES strings).<sup>11</sup> Note that these structures don't include 3D coordinates, since solubility is a property of a molecule and not of its particular conformers.

## **FreeSolv**

The Free Solvation Database (FreeSolv) provides experimental and calculated hydration free energy of small molecules in water.<sup>9</sup> A subset of the compounds in the dataset are also used in the SAMPL blind prediction challenge.<sup>31</sup> The calculated values are derived from alchemical free energy calculations using molecular dynamics simulations. We include the experimental values in the benchmark collection, and use calculated values for comparison.

## **PCBA**

As mentioned previously, PubChem BioAssay (PCBA) is a database consisting of biological activities of small molecules generated by high-throughput screening.<sup>24</sup> We use a subset of PCBA, containing 128 bioassays measured over 400,000 compounds, used by previous work to benchmark machine learning methods.<sup>3</sup>

## **MUV**

The Maximum Unbiased Validation (MUV) group is another benchmark dataset selected from PubChem BioAssay by applying a refined nearest neighbor analysis.<sup>32</sup> The MUV



dataset contains 17 challenging tasks for around 90,000 compounds and is specifically designed for validation of virtual screening techniques.

## **PDBbind**

PDBbind is a comprehensive database of experimentally measured binding affinities for biomolecular complexes.<sup>33,34</sup> Unlike other ligand-based biological activity datasets, in which only the structures of ligands are provided, PDBbind provides detailed 3D Cartesian coordinates of both ligands and their target proteins derived from experimental (e.g., X-Ray crystallography) measurements. The availability of coordinates of the protein-ligand complexes permits structure-based featurization that is aware of the protein-ligand binding geometry. We use the “refined” and “core” subsets of the database,<sup>35</sup> more carefully processed for data artifacts, as additional benchmarking targets.

## **HIV**

The HIV dataset was introduced by the Drug Therapeutics Program (DTP) AIDS Antiviral Screen, which tested the ability to inhibit HIV replication for over 40,000 compounds.<sup>36</sup> Screening results were evaluated and placed into three categories: confirmed inactive (CI), confirmed active (CA) and confirmed moderately active (CM). We further combine the latter two labels, making it a classification task between inactive (CI) and active (CA and CM).

## **Tox21**

The “Toxicology in the 21st Century” (Tox21) initiative created a public database measuring toxicity of compounds, which has been used in the 2014 Tox21 Data Challenge.<sup>37</sup> This dataset contains qualitative toxicity measurements for 8014 compounds on 12 different targets, including nuclear receptors and stress response pathways.

## **ToxCast**

ToxCast is another data collection (from the same initiative as Tox21) providing toxicology data for a large library of compounds based on *in vitro* high-throughput screening.<sup>38</sup> The processed collection in MoleculeNet includes qualitative results of over 600 experiments on 8615 compounds.

## **SIDER**

The Side Effect Resource (SIDER) is a database of marketed drugs and adverse drug reactions (ADR).<sup>39</sup> The version of the SIDER dataset in DeepChem<sup>40</sup> has grouped drug side-effects into 27 system organ classes following MedDRA classifications<sup>41</sup> measured for 1427 approved drugs (following previous usage<sup>42</sup>).

## **ClinTox**

The ClinTox dataset, introduced as part of this work, addresses clinical drug toxicity by providing a qualitative comparison of drugs approved by the FDA and those that have failed clinical trials for toxicity reasons.<sup>43,44</sup> The dataset is comprised of two classification tasks: clinical trial toxicity (or absence of toxicity) and FDA approval status, for 1491 drug compounds with known chemical structure.

## **Dataset splitting**

As mentioned previously, machine learning methods require datasets to be split into training/validation/test subsets (or alternatively into  $K$ -folds) for benchmarking. All MoleculeNet datasets are split into training, validation and test, following a 80/10/10 ratio. Training sets were used to train models, while validation sets were used for tuning hyperparameters, and test sets were used for evaluation of models. To facilitate comparison, performances of models on different datasets share the same settings tuned by hyperparameter search across all datasets.

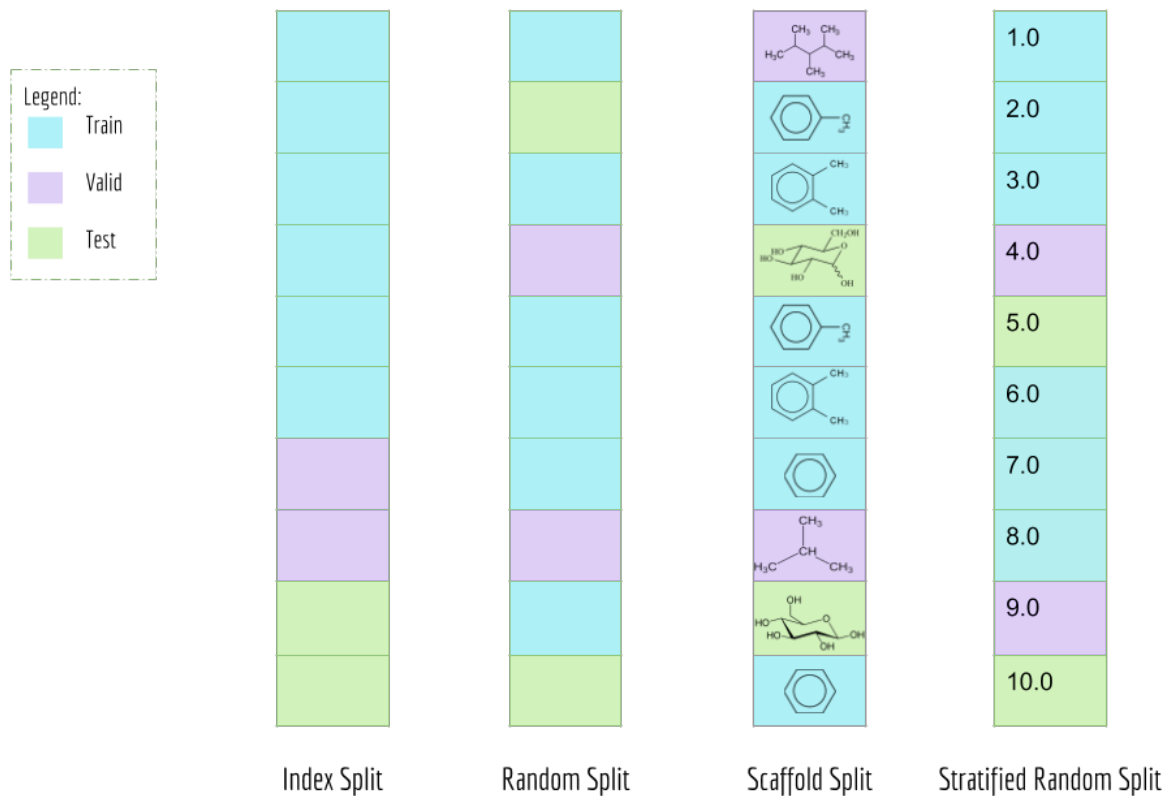


Figure 3: Representation of Data Splits in MoleculeNet

As mentioned previously, random splitting of molecular data isn't always best for evaluating machine learning methods. Consequently, MoleculeNet implements multiple different splittings for each dataset. Index splitting directly separates samples based on their order, namely using the first 80% to train and the rest to validate and test. This splitting method depends on the arbitrary order in which the dataset was originally listed, yet can be useful at times as a counterpoint to more sophisticated splitting mechanisms. Random splitting randomly splits samples into the train/valid/test subsets. Scaffold splitting splits the samples based on their two-dimensional structural frameworks,<sup>45</sup> as implemented in RDKit.<sup>46</sup> Since scaffold splitting attempts to separate structurally molecules in the training/validation/test sets, the scaffold split offers a greater challenge for learning algorithms than the random split.

In addition, a stratified random sampling method is implemented on the QM7/QM7b datasets to reproduce the results from the original work.<sup>8</sup> This method sorts datapoints in order of increasing label value (note this is only defined for real-valued output). This sorted list is then split into train/valid/test by ensuring that each set contains the full range of provided labels.

MoleculeNet contributes the code for these splitting methods into DeepChem. Users of the library can use these splits on new datasets with short library calls.

## Metrics

MoleculeNet contains both regression datasets (QM7, QM7b, ESOL, FreeSolv and PDBbind) and classification datasets (PCBA, MUV, HIV, Tox21, ToxCast, SIDER and ClinTox), thus requiring different performance metrics to be measured on each task. Following suggestions from previous work,<sup>47</sup> regression datasets are evaluated by squared Pearson correlation coefficient ( $R^2$ ), and classification datasets are evaluated by area under curve (AUC) of the receiver operating characteristic (ROC) curve.<sup>48</sup> For datasets containing more than one task, we report the mean metric values over all tasks.

## Featurization

A core challenge for molecular machine learning is effectively encoding molecules into fixed-length strings or vectors. Although SMILES strings are unique representations of molecules, most molecular machine learning methods require further information to learn sophisticated electronic or topological features of molecules from limited amounts of data. (Recent work has demonstrated the ability to learn useful representations from SMILES strings using more sophisticated methods,<sup>49</sup> so it may be feasible to use SMILES strings for further learning tasks in the near future.) Furthermore, the enormity of chemical space often requires representations of molecules specifically suited to the learning task at hand. MoleculeNet contains implementations of four useful molecular featurization methods.

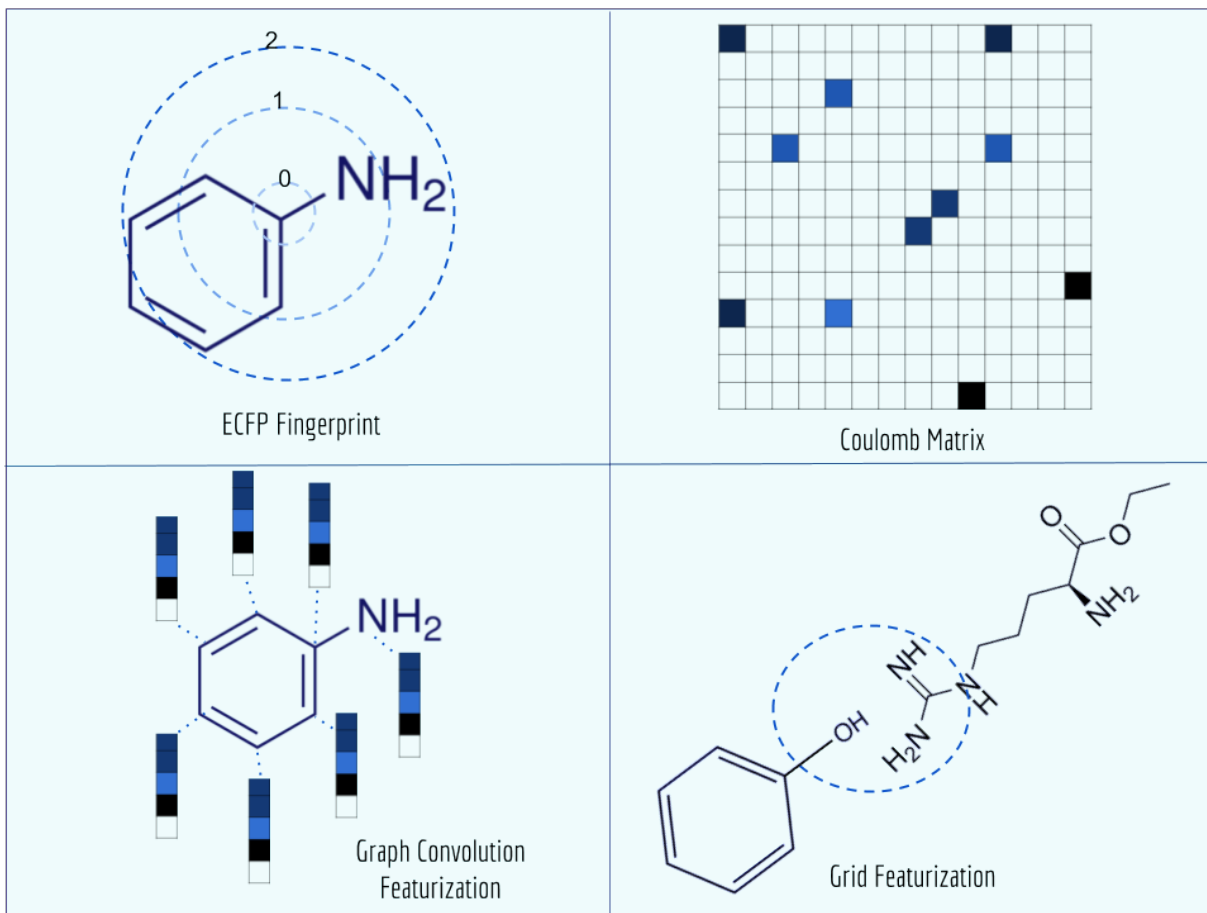


Figure 4: Diagrams of featurizations in MoleculeNet.

## ECFP

Extended-Connectivity Fingerprints (ECFP) are widely-used molecular characterizations in chemical informatics.<sup>10</sup> During the featurization process, a molecule is decomposed into submodules originated from heavy atoms, each assigned with a unique identifier. These segments and identifiers are extended through bonds to generate larger substructures and corresponding identifiers.

After hashing all these substructures into a fixed length binary fingerprint, the representation contains information about topological characteristics of the molecule, which enables it to be applied to tasks such as similarity searching and activity prediction. The MoleculeNet implementation uses ECFP4 fingerprints generated by RDKit.<sup>46</sup>

## Graph Convolutions

Graph convolutions extend the decomposition principles of ECFP. Both methods gradually merge information for distant atoms by extending radially through bonds. This information is used to generate identifiers for all substructures. However, instead of applying fixed hash functions, graph convolutional models use learnable network layers to implement the featurization process.<sup>11</sup> Using a smooth and differentiable function allows the model to learn weights through back propagation. More generally, graph convolutional models regard molecules as undirected graphs, and apply the same (learnable) function to every node (atom) in the graph. This structure recapitulates convolution layers in visual recognition deep networks.

The graph convolutional featurization computes an initial feature vector for each atom that summarizes its local chemical environment. This includes features such as atom-type, hybridization types, and valence structures. These initial feature vectors are fed into graph convolutional networks (discussed in further detail later).

We note briefly that there are multiple variants of graph convolutional networks. MoleculeNet currently implements only one such algorithm,<sup>11</sup> but additional variants may be added in the future.

## Coulomb Matrix

*Ab-initio* electronic structure calculations typically require a set of nuclear charges  $\{Z\}$  and the corresponding Cartesian coordinates  $\{\mathbf{R}\}$  as input. The Coulomb Matrix  $\mathbf{M}$ , proposed by Rupp et al.<sup>7</sup> and defined below, encodes this information by use of the atomic self-energies and internuclear Coulomb repulsion operator.

$$M_{IJ} = \begin{cases} 0.5Z_I^2 & \text{for } I = J \\ \frac{Z_I Z_J}{|\mathbf{R}_I - \mathbf{R}_J|} & \text{for } I \neq J \end{cases}$$

Here, the off-diagonal elements correspond to the Coulomb repulsion between atoms  $I$

and J, and the diagonal elements correspond to a polynomial fit of atomic self-energy to nuclear charge. The Coulomb Matrix of a molecule is invariant to translation and rotation of that molecule, but not with respect to atom index permutation. In the construction of coulomb matrix, we first use the nuclear charges and distance matrix generated by RDKit<sup>46</sup> to acquire the original coulomb matrix, then apply the random atom index sorting and binary expansion transformations to it during training, as reported by Montavon et al.<sup>8</sup>

## Grid Featurizer

The grid featurizer is a featurization method (introduced in the current work) initially designed for the PDDBind dataset in which structural information of both the ligand and target protein are considered. Since binding affinity stems largely from the intermolecular forces between ligands and proteins, in addition to intramolecular interactions, we seek to incorporate both the chemical interaction within the binding pocket as well as features of the protein and ligand individually.

The grid featurizer was inspired by the NNscore featurizer<sup>50</sup> and SPLIF<sup>51</sup> but optimized for speed, robustness, and generalizability. The intermolecular interactions enumerated by the featurizer include salt bridges and hydrogen bonding between protein and ligand, intra-ligand circular fingerprints, intra-protein circular fingerprints, and protein-ligand SPLIF fingerprints.

## Models

MoleculeNet tests the performance of various machine learning models on the datasets discussed previously. The following sections will give brief introductions to benchmarked algorithms. The next section will discuss performance numbers in detail. Here we briefly review logistic regression, random forests, multitask networks,<sup>2,3</sup> bypass networks,<sup>52</sup> influence relevance voting<sup>53</sup> and graph convolution models.<sup>11</sup> Figure 5 illustrates some of these methods. As part of this work, all methods are implemented in the open source DeepChem

package.<sup>19</sup> (The logistic regression and influence relevance voting methods were implemented specifically for MoleculeNet; the other algorithms were already implemented in DeepChem previously.)



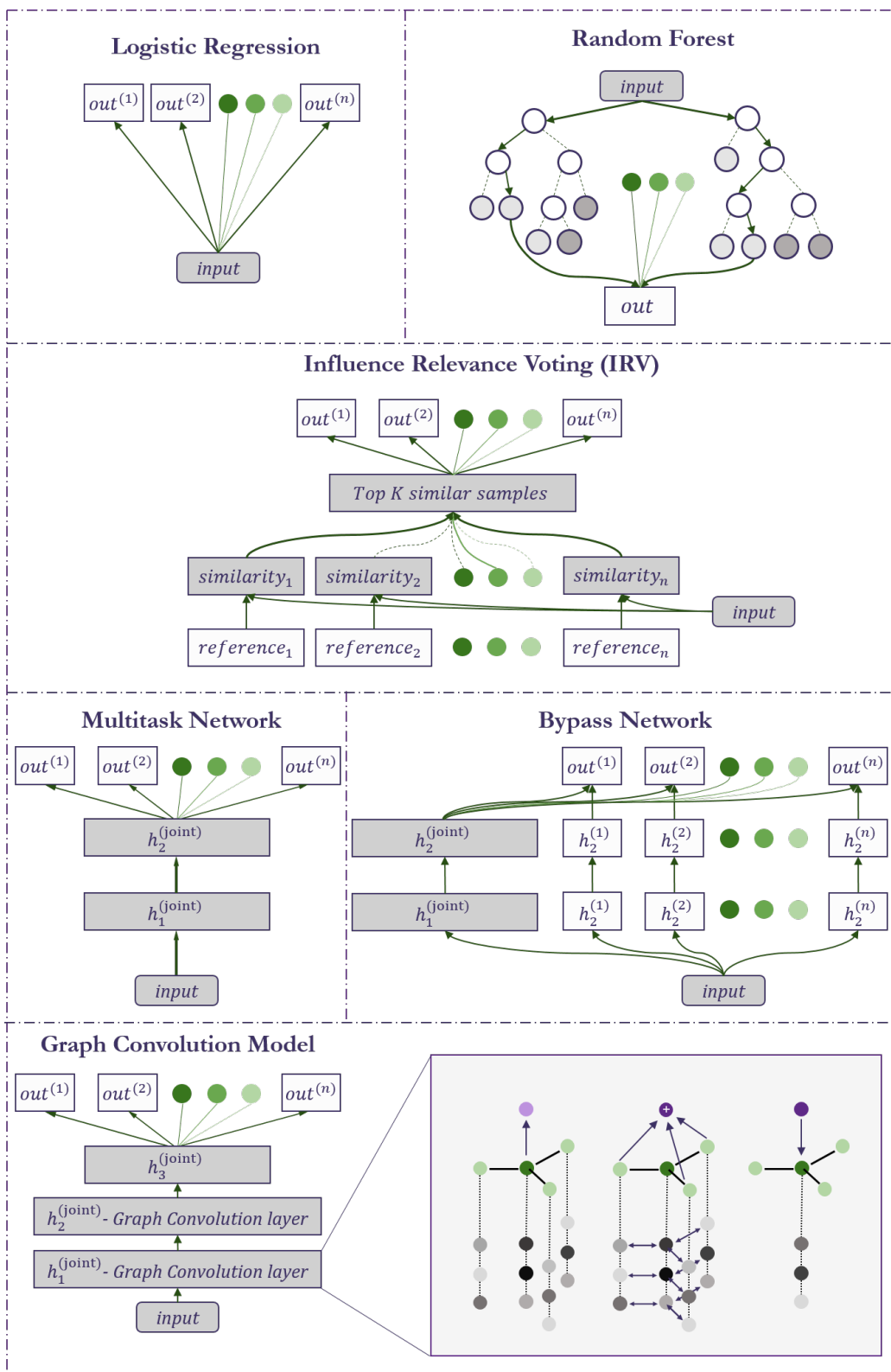


Figure 5: Diagrams of models implemented in MoleculeNet

## Logistic Regression

Logistic regression models apply the logistic function to weighted linear combinations of their input features to obtain model predictions. It is often common to use regularization to encourage learned weights to be sparse.<sup>54</sup> Note that logistic regression models are only defined for classification tasks.

## Random Forests

Random forests are ensemble prediction methods.<sup>55</sup> A random forest consists of many individual decision trees, each of which is trained on a subsampled version of the original dataset. The results for individual trees are averaged to provide output predictions for the full forest. Random forests can be used for both classification and regression tasks. Training a random forest can be computationally intensive, so benchmarks only include random forest results for smaller datasets.

## Multitask Network

In a multitask network,<sup>3</sup> input featurizations are processed by fully connected neural network layers. The processed output is shared among all learning tasks in a dataset, and then fed into separate linear classifiers/regressors for each different task. In the case that a dataset contains only a single task, multitask networks are just fully connected neural networks. Since multitask networks train on the joint data available for various tasks, the parameters of the shared layers are encouraged to produce a joint representation which can share information between learning tasks. This effect does seem to have limitations; merging data from uncorrelated tasks has only moderate effect.<sup>56</sup> As a result, MoleculeNet does not attempt to train extremely large multitask networks combining all data for all datasets.

## Bypass Multitask Networks

Multitask modeling relies on the fact that some features have explanatory power that is shared among multiple tasks. Note that the opposite may well be true; features useful for one task can be detrimental to other tasks. As a result, vanilla multitask networks can lack the power to explain unrelated variations in the samples. Bypass networks attempt to overcome this variation by merging in per-task independent layers that “bypass” shared layers to directly connect inputs with outputs.<sup>57</sup> In other words, bypass multitask networks consist of  $n_{\text{tasks}} + 1$  independent components: one “multitask” layers mapping all inputs to shared representations, and  $n_{\text{tasks}}$  “bypass” layers mapping inputs for each specific task to their labels. As the two groups have separate parameters, bypass networks may have greater explanatory power than vanilla multitask networks.

## Influence Relevance Voting

Influence Relevance Voting (IRV) systems are refined K-nearest neighbour classifiers.<sup>53</sup> Using the hypothesis that compounds with similar substructures have similar functionality, the IRV classifier makes its prediction by combining labels from the top- $K$  compounds most similar to a provided test sample.

The Jaccard-Tanimoto similarity between fingerprints of compounds is used as the similarity measurement:

$$S(\vec{A}, \vec{B}) = \frac{A \cap B}{A \cup B}$$

The IRV model then calculates a weighted sum of labels of top K similar compounds to predict the result, in which weights are the outputs of a one-hidden layer neural network with similarities and rankings of K similar compounds as input. Detailed descriptions of the model can be found in the original article.<sup>53</sup>

## Graph Convolution models

As mentioned previously, graph convolutional models directly use connectivity graphs of molecules as inputs. In particular, graph convolutional models provide a learnable featurization process capable of extracting useful representations of molecules suited to the task at hand. (Note that this property is shared, to some degree, by all deep architectures considered in MoleculeNet. However, graph convolutional architectures are more explicitly designed to encourage extraction of useful featurizations).

MoleculeNet uses the graph convolutional implementation in DeepChem from previous work.<sup>42</sup> This implementation converts SMILES strings into molecular graphs using RDKit<sup>46</sup> As mentioned previously, the initial representations assigns to each atom a vector of features including its element, connectivity, valence, etc. Then several graph convolutions, each consisting of a graph convolution layer, a batch normalization layer and a graph pool layer, are sequentially added, followed by a fully-connected dense layer. Finally, the feature vectors for all nodes (atoms) are summed, generating a graph feature vector, which is fed to a classification or regression layer.

Note that graph convolutional models can be multitask (the extracted graph feature vector can be shared for many learning tasks).

## Results and Discussion

In this section, we discuss the performance of benchmarked models on MoleculeNet datasets. For classification tasks, we include results for multitask networks, bypass networks, IRV, and graph convolution models. The multitask, bypass and IRV models use ECFP featurizations of input. Per-task ECFP-featurized logistic regression and random forest results are also included to serve as baseline comparisons.

For regression tasks, results of ECFP-featurized multitask networks and graph convolutional models are reported, together with random forest baselines. For QM7/QM7b and

PDBbind, performances based on different Coulomb and Grid featurizations respectively are also included and compared.

## Physiology and biophysics tasks

Tables 2, 3 and 4 report ROC-AUC results of 4 to 6 different models on biophysical datasets (PCBA, MUV, HIV) and physiological datasets (SIDER, Toxcast, Tox21, ClinTox). All of these datasets contain only classification tasks.

Most models have train scores higher than valid/test scores, indicating that overfitting is a general issue. Singletask logistic regression exhibits the largest gaps between train scores and valid/test scores, while models incorporating multitask structure generally show less overfit, suggesting that multitask training has a regularizing effect. Most physiological and biophysical datasets in MoleculeNet have only a low volume of data for each task. Multitask algorithms combine different tasks, resulting in a larger pool of data for model training. In particular, multitask training can, to a some extent, compensate for the limited data amount available for each individual task.

Bypass networks have higher train scores and a slightly lower valid/test scores compared with vanilla multitask networks, suggesting that the bypass structure does not add much explanatory power. This may be due to the high homogeneity of tasks within each dataset. IRV models achieve performance broadly comparable with multitask networks. However, the quadratic nearest neighbor search makes the IRV models slower to train than the multitask networks.

Graph convolutional models, based on a continuous and adaptive version of fingerprinting,<sup>11</sup> show strong valid/test results on almost all datasets, along with less overfit. Similar results are reported in previous graph-convolutional algorithms,<sup>11,12</sup> showing that learnable featurizations can provide a large boost compared with conventional featurizations like ECFP.

Comparing the three different splitting patterns, index and random splits show compa-

rable valid/test results, while scaffold valid/test results are significantly lower. As expected, scaffold splitting divides compounds by their molecular scaffolds, increasing the difference between the train, valid and test sets. Scaffold splits provide a stronger test of a given model’s generalizability compared with index and random splits. The graph convolutions tend to have the strongest performance even with scaffold splits.

Another interesting result that worth mentioning is the poorer performances of models on physiological datasets, such as SIDER and ToxCast. This poor performance could possibly be explained by the relatively small amount of data in the two sets. But more likely, predicting side effects and toxicology are tasks that require greater explanatory power than current models possess due to the complexity of the human body. Using a more specialized featurization method or additional sources of data may improve the situation, but a fuller investigation is left to future research.

Table 2: Performances with Index Splitter (AUC-ROC)

| Dataset | Model               | Mean Train | Mean Valid   | Mean Test    |
|---------|---------------------|------------|--------------|--------------|
| Tox21   | Logistic Regression | 0.903      | 0.704        | 0.738        |
|         | Random Forest       | 0.999      | 0.734        | 0.769        |
|         | IRV                 | 0.811      | 0.767        | 0.789        |
|         | Multitask           | 0.856      | 0.763        | 0.781        |
|         | Bypass              | 0.851      | 0.761        | 0.775        |
|         | Graph Convolution   | 0.899      | <b>0.812</b> | <b>0.810</b> |
| MUV     | Logistic Regression | 0.960      | 0.773        | 0.717        |
|         | Multitask           | 0.907      | 0.755        | 0.767        |
|         | Bypass              | 0.940      | 0.761        | 0.715        |
|         | Graph Convolution   | 0.891      | <b>0.815</b> | <b>0.786</b> |
| PCBA    | Logistic Regression | 0.809      | 0.776        | 0.781        |
|         | Multitask           | 0.821      | 0.776        | 0.781        |
|         | Bypass              | 0.814      | 0.785        | 0.782        |
|         | Graph Convolution   | 0.877      | <b>0.848</b> | <b>0.845</b> |
| SIDER   | Logistic Regression | 0.931      | 0.622        | 0.602        |
|         | Random Forest       | 0.999      | <b>0.670</b> | <b>0.644</b> |
|         | IRV                 | 0.649      | 0.642        | 0.580        |
|         | Multitask           | 0.778      | 0.631        | 0.612        |
|         | Bypass              | 0.807      | 0.639        | 0.617        |
|         | Graph Convolution   | 0.751      | 0.613        | 0.585        |
| ToxCast | Logistic Regression | 0.727      | 0.578        | 0.464        |
|         | Multitask           | 0.829      | 0.675        | 0.664        |
|         | Bypass              | 0.824      | 0.677        | 0.671        |
|         | Graph Convolution   | 0.845      | <b>0.722</b> | <b>0.707</b> |
| ClinTox | Logistic Regression | 0.968      | 0.676        | 0.651        |
|         | Random Forest       | 0.995      | 0.776        | 0.623        |
|         | IRV                 | 0.763      | 0.814        | 0.736        |
|         | Multitask           | 0.935      | 0.830        | <b>0.824</b> |
|         | Bypass              | 0.950      | 0.827        | 0.810        |
|         | Graph Convolution   | 0.927      | <b>0.865</b> | 0.745        |
| HIV     | Logistic Regression | 0.864      | 0.739        | 0.741        |
|         | Random Forest       | 0.999      | 0.720        | 0.733        |
|         | IRV                 | 0.841      | 0.724        | <b>0.750</b> |
|         | Singletask          | 0.761      | 0.652        | 0.617        |
|         | Bypass              | 0.780      | 0.708        | 0.727        |
|         | Graph Convolution   | 0.876      | <b>0.779</b> | 0.712        |

Table 3: Performances with Random Splitter (AUC-ROC)

| Dataset | Model               | Mean Train | Mean Valid   | Mean Test    |
|---------|---------------------|------------|--------------|--------------|
| Tox21   | Logistic Regression | 0.901      | 0.742        | 0.755        |
|         | Random Forest       | 0.999      | 0.763        | 0.758        |
|         | IRV                 | 0.807      | 0.775        | 0.787        |
|         | Multitask           | 0.850      | 0.777        | 0.799        |
|         | Bypass              | 0.845      | <b>0.811</b> | 0.820        |
|         | Graph Convolution   | 0.898      | <b>0.811</b> | <b>0.848</b> |
| MUV     | Logistic Regression | 0.954      | 0.780        | 0.740        |
|         | Multitask           | 0.904      | 0.687        | 0.769        |
|         | Bypass              | 0.945      | 0.790        | <b>0.788</b> |
|         | Graph Convolution   | 0.908      | <b>0.876</b> | <b>0.788</b> |
| PCBA    | Logistic Regression | 0.808      | 0.772        | 0.773        |
|         | Multitask           | 0.815      | 0.797        | 0.788        |
|         | Bypass              | 0.813      | 0.780        | 0.780        |
|         | Graph Convolution   | 0.878      | <b>0.848</b> | <b>0.847</b> |
| SIDER   | Logistic Regression | 0.933      | 0.632        | 0.622        |
|         | Random Forest       | 0.999      | 0.691        | <b>0.697</b> |
|         | IRV                 | 0.649      | 0.613        | 0.640        |
|         | Multitask           | 0.780      | <b>0.695</b> | 0.626        |
|         | Bypass              | 0.802      | 0.646        | 0.618        |
|         | Graph Convolution   | 0.739      | 0.652        | 0.638        |
| ToxCast | Logistic Regression | 0.713      | 0.538        | 0.557        |
|         | Multitask           | 0.827      | 0.669        | 0.685        |
|         | Bypass              | 0.831      | 0.657        | 0.697        |
|         | Graph Convolution   | 0.848      | <b>0.707</b> | <b>0.719</b> |
| ClinTox | Logistic Regression | 0.972      | 0.726        | 0.764        |
|         | Random Forest       | 0.997      | 0.670        | 0.580        |
|         | IRV                 | 0.787      | 0.807        | 0.692        |
|         | Multitask           | 0.951      | <b>0.834</b> | <b>0.883</b> |
|         | Bypass              | 0.960      | 0.831        | 0.838        |
|         | Graph Convolution   | 0.976      | <b>0.834</b> | 0.848        |
| HIV     | Logistic Regression | 0.860      | 0.806        | 0.809        |
|         | Random Forest       | 0.999      | <b>0.850</b> | 0.818        |
|         | IRV                 | 0.839      | 0.809        | 0.798        |
|         | Singletask          | 0.742      | 0.715        | 0.732        |
|         | Bypass              | 0.753      | 0.727        | 0.716        |
|         | Graph Convolution   | 0.847      | 0.803        | <b>0.830</b> |



Table 4: Performances with Scaffold Splitter (AUC-ROC)

| Dataset | Model               | Mean Train | Mean Valid   | Mean Test    |
|---------|---------------------|------------|--------------|--------------|
| Tox21   | Logistic Regression | 0.905      | 0.651        | 0.697        |
|         | Random Forest       | 0.999      | 0.629        | 0.701        |
|         | IRV                 | 0.823      | 0.708        | 0.701        |
|         | Multitask           | 0.861      | 0.710        | 0.741        |
|         | Bypass              | 0.863      | 0.712        | 0.740        |
|         | Graph Convolution   | 0.901      | <b>0.730</b> | <b>0.771</b> |
| MUV     | Logistic Regression | 0.956      | 0.702        | 0.712        |
|         | Multitask           | 0.909      | 0.730        | 0.693        |
|         | Bypass              | 0.948      | 0.724        | 0.716        |
|         | Graph Convolution   | 0.893      | <b>0.742</b> | <b>0.734</b> |
| PCBA    | Logistic Regression | 0.811      | 0.746        | 0.757        |
|         | Multitask           | 0.816      | 0.764        | 0.765        |
|         | Bypass              | 0.818      | 0.758        | 0.759        |
|         | Graph Convolution   | 0.883      | <b>0.822</b> | <b>0.821</b> |
| SIDER   | Logistic Regression | 0.926      | 0.592        | 0.622        |
|         | Random Forest       | 0.999      | <b>0.620</b> | 0.632        |
|         | IRV                 | 0.639      | 0.599        | <b>0.648</b> |
|         | Multitask           | 0.778      | 0.557        | 0.626        |
|         | Bypass              | 0.797      | 0.556        | 0.627        |
|         | Graph Convolution   | 0.753      | 0.576        | 0.615        |
| ToxCast | Logistic Regression | 0.717      | 0.496        | 0.496        |
|         | Multitask           | 0.827      | 0.609        | 0.603        |
|         | Bypass              | 0.831      | <b>0.614</b> | 0.612        |
|         | Graph Convolution   | 0.861      | 0.609        | <b>0.620</b> |
| ClinTox | Logistic Regression | 0.960      | 0.803        | 0.694        |
|         | Random Forest       | 0.993      | 0.735        | 0.687        |
|         | IRV                 | 0.787      | 0.807        | 0.692        |
|         | Multitask           | 0.948      | 0.862        | <b>0.777</b> |
|         | Bypass              | 0.953      | <b>0.890</b> | 0.774        |
|         | Graph Convolution   | 0.964      | 0.830        | 0.710        |
| HIV     | Logistic Regression | 0.858      | 0.798        | 0.738        |
|         | Random Forest       | 0.946      | 0.562        | 0.539        |
|         | IRV                 | 0.847      | <b>0.811</b> | 0.735        |
|         | Singletask          | 0.775      | 0.765        | 0.726        |
|         | Bypass              | 0.785      | 0.748        | 0.673        |
|         | Graph Convolution   | 0.867      | 0.769        | <b>0.752</b> |

## ESOL and FreeSolv

Solubility and solvation free energy are two basic physical chemistry properties important for understanding how molecules interact with solvents such as water. As listed in Table 5, all tested models achieve reasonable performance predicting these properties. As before, graph convolutional methods exhibit a significant boost, indicating the advantages of learnable featurizations.

Table 5: ESOL and FreeSolve Performances ( $R^2$ )

| Dataset  | Model             | Splitting | Train | Valid        | Test         |
|----------|-------------------|-----------|-------|--------------|--------------|
| ESOL     | Random Forest     | Index     | 0.953 | 0.626        | 0.676        |
|          | Singletask        | Index     | 0.868 | 0.578        | 0.629        |
|          | Graph Convolution | Index     | 0.967 | <b>0.790</b> | <b>0.829</b> |
|          | Random Forest     | Random    | 0.951 | 0.684        | 0.704        |
|          | Singletask        | Random    | 0.865 | 0.574        | 0.619        |
|          | Graph Convolution | Random    | 0.964 | <b>0.782</b> | <b>0.823</b> |
|          | Random Forest     | Scaffold  | 0.953 | 0.284        | 0.487        |
|          | Singletask        | Scaffold  | 0.866 | 0.342        | 0.418        |
|          | Graph Convolution | Scaffold  | 0.967 | <b>0.606</b> | <b>0.629</b> |
| FreeSolv | Random Forest     | Index     | 0.968 | 0.736        | 0.841        |
|          | Singletask        | Index     | 0.917 | 0.764        | 0.850        |
|          | Graph Convolution | Index     | 0.982 | <b>0.864</b> | <b>0.920</b> |
|          | Random Forest     | Random    | 0.968 | 0.612        | 0.762        |
|          | Singletask        | Random    | 0.908 | 0.830        | 0.682        |
|          | Graph Convolution | Random    | 0.987 | <b>0.868</b> | <b>0.838</b> |
|          | Random Forest     | Scaffold  | 0.965 | 0.473        | 0.256        |
|          | Singletask        | Scaffold  | 0.891 | 0.217        | 0.252        |
|          | Graph Convolution | Scaffold  | 0.985 | <b>0.666</b> | <b>0.503</b> |

One interesting comparison here is how data-driven method competes with *ab-initio* calculations. Hydration free energy has been widely used as a test of computational chemistry methods. With free energy values ranging from -25.5 to 3.4kcal/mol in the FreeSolv dataset, RMSE for calculated results reach up to 1.5kcal/mol.<sup>31</sup> On the other hand, though machine learning methods typically need large amounts of training data to acquire predictive power, they can achieve higher accuracies given enough data. We investigate how the performance of machine learning methods on FreeSolve changes with the volume of training data. In

particular, we want to know the amount of data required for machine learning to achieve accuracy similar to that of physically inspired algorithms.

For Figure 6, we generated a series of models with different training set volumes (represented as fractions of the whole dataset) and calculated their out-of-sample RMSE. Each data point displayed is the average of 10 independent runs, with standard deviations displayed as error bars. Surprisingly, graph convolutional models are capable of achieving comparable results with physical methods when given enough training data. The FreeSolve dataset only contains around 600 compounds. When roughly 500 samples are provided for training (fraction  $\sim 0.8$ ), graph convolution achieves accuracies comparable to that of physical methods.

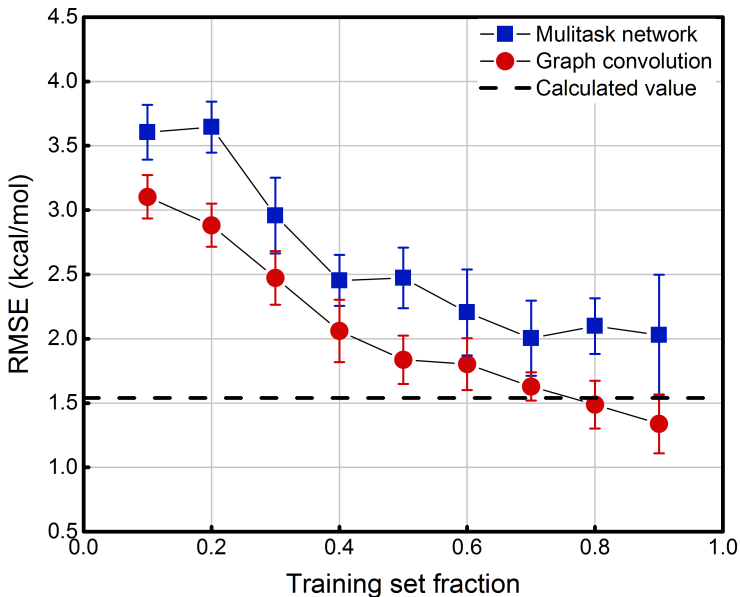


Figure 6: Out-of-sample performances of models with different training set fractions. Each data point displayed is the average of 10 independent runs, with standard deviations shown as error bars.

## PDBbind

PDBBind maps distinct ligand-protein structures to their binding affinities. As discussed in the datasets section, we created Grid Featurizer to harness the joint ligand-protein structural information in PDBBind to build a model that predicts the experimental  $K_i$  of binding. All results listed in Table 6 use random splitting (The original dataset is sorted in order of increasing activity, so index splitting yields very poor models. Scaffold splits don't account for protein diversity and aren't as meaningful as for ligand-only datasets). Table 6 displays results for the core, refined, and full subsets of PDBbind. (Core contains roughly 200 structures, refined 4000, and full 15000. The smaller datasets are cleaned more thoroughly than larger datasets.) Singletask networks and random forests based on the grid featurization achieve reasonably strong valid/test set performance, while the ligand baselines (which ignore protein structure) achieve much weaker performance. Note that models on the full set aren't significantly superior to models with less data; this effect may be due to the additional data being less clean.

Note that all models display heavy overfitting. Additional clean data may be required to create more accurate models for protein-ligand binding.

Table 6: PDBbind Performances ( $R^2$ )

| Dataset           | Model                     | Train | Valid        | Test         |
|-------------------|---------------------------|-------|--------------|--------------|
| PDBbind (core)    | Singletask (ECFP)         | 0.770 | 0.425        | 0.245        |
|                   | Graph Convolution (graph) | 0.749 | 0.136        | <b>0.348</b> |
|                   | Random Forest (grid)      | 0.969 | <b>0.445</b> | 0.326        |
|                   | Singletask (grid)         | 0.987 | 0.311        | 0.205        |
| PDBbind (refined) | Singletask (ECFP)         | 0.766 | 0.350        | 0.406        |
|                   | Graph Convolution (graph) | 0.661 | 0.445        | 0.469        |
|                   | Random Forest (grid)      | 0.963 | <b>0.511</b> | <b>0.472</b> |
|                   | Singletask (grid)         | 0.984 | 0.462        | 0.420        |
| PDBbind (full)    | Singletask (ECFP)         | 0.373 | 0.361        | 0.337        |
|                   | Graph Convolution (graph) | 0.193 | 0.196        | 0.189        |
|                   | Random Forest (grid)      | 0.965 | <b>0.493</b> | <b>0.484</b> |
|                   | Singletask (grid)         | 0.960 | 0.488        | 0.471        |

## QM7 and QM7b

The QM7/QM7b datasets represent another distinct category of properties that are typically calculated through solving Schrödinger’s equation (approximately using techniques such as DFT). As most conventional methods are slower than data-driven methods by orders of magnitude, we hope to learn effective approximators by training on existing datasets.

Table 7 and 8 display the performances of ECFP-based multitask networks, random forests and graph convolution models, together with multitask networks using Coulomb featurization. Note that that only the Coulomb-based methods use the 3D geometry of compounds, which are expected to be critical for accurate prediction of quantum properties. Unsurprisingly, Coulomb-featurized multitask networks exhibit much less overfitting and outperform the other three models by a large margin. When using the same splitting strategy as reported by previous work,<sup>8</sup> mean absolute error performances on the task of predicting atomization energy reaches similar accuracy as reported in previous work on this dataset. (There is still a gap between the MoleculeNet implementation and best reported numbers from previous work,<sup>8</sup> which would likely be closed by training models longer).

For QM7/QM7b, proper choice of featurization appears critical. As mentioned previously, ECFP and graph featurizations only consider graph substructures, while Coulomb featurizations explicitly calculate the charges and Coulomb potentials, which are exactly the required input for solving Schrödinger’s equation.

Table 7: QM7 Performances ( $R^2$ )

| Dataset | Model                       | Splitting  | Train | Valid        | Test         |
|---------|-----------------------------|------------|-------|--------------|--------------|
| QM7     | Random Forest (ECFP)        | Index      | 0.942 | 0.724        | 0.704        |
|         | Singletask (ECFP)           | Index      | 0.990 | 0.806        | 0.752        |
|         | Graph Convolution (graph)   | Index      | 0.979 | 0.956        | 0.946        |
|         | Singletask (Coulomb Matrix) | Index      | 0.997 | <b>0.986</b> | <b>0.983</b> |
|         | Random Forest (ECFP)        | Random     | 0.947 | 0.575        | 0.572        |
|         | Singletask (ECFP)           | Random     | 0.991 | 0.752        | 0.745        |
|         | Graph Convolution (graph)   | Random     | 0.984 | 0.967        | 0.938        |
|         | Singletask (Coulomb Matrix) | Random     | 0.999 | <b>0.999</b> | <b>0.999</b> |
|         | Random Forest (ECFP)        | Stratified | 0.946 | 0.562        | 0.539        |
|         | Singletask (ECFP)           | Stratified | 0.993 | 0.790        | 0.765        |
|         | Graph Convolution (graph)   | Stratified | 0.982 | 0.937        | 0.936        |
|         | Singletask (Coulomb Matrix) | Stratified | 0.999 | <b>0.999</b> | <b>0.999</b> |
| QM7b    | Multitask (Coulomb Matrix)  | Index      | 0.931 | 0.803        | 0.454        |
|         | Multitask (Coulomb Matrix)  | Random     | 0.923 | 0.884        | 0.880        |
|         | Multitask (Coulomb Matrix)  | Stratified | 0.934 | 0.884        | 0.884        |

Table 8: QM7 Performances (Mean Absolute Error/kcal · mol<sup>-1</sup>)

| Dataset | Model                       | Splitting  | Train | Valid       | Test        |
|---------|-----------------------------|------------|-------|-------------|-------------|
| QM7     | Random Forest (ECFP)        | Index      | 41.9  | 82.6        | 124         |
|         | Singletask (ECFP)           | Index      | 13.2  | 63.4        | 94.0        |
|         | Graph Convolution (ECFP)    | Index      | 16.0  | 26.7        | 39.8        |
|         | Singletask (Coulomb Matrix) | Index      | 11.0  | <b>12.0</b> | <b>22.7</b> |
|         | Random Forest (ECFP)        | Random     | 39.5  | 107         | 103         |
|         | Singletask (ECFP)           | Random     | 11.9  | 84.0        | 74.6        |
|         | Graph Convolution (ECFP)    | Random     | 14.1  | 28.4        | 31.8        |
|         | Singletask (Coulomb Matrix) | Random     | 7.12  | <b>7.53</b> | <b>7.45</b> |
|         | Random Forest (ECFP)        | Stratified | 38.8  | 109         | 107         |
|         | Singletask (ECFP)           | Stratified | 12.1  | 83.5        | 81.2        |
|         | Graph Convolution (ECFP)    | Stratified | 15.4  | 31.3        | 31.1        |
|         | Singletask (Coulomb Matrix) | Stratified | 6.61  | <b>7.34</b> | <b>7.21</b> |

## Conclusion

This work introduces MoleculeNet, a benchmark for molecular machine learning. We gathered data for a wide range of molecular properties: 12 dataset collections including over 800 different tasks on 600,000 compounds. Tasks are categorized into 4 levels as illustrated

in Figure 2: (i) atomic-level quantum mechanical characters; (ii) molecular-level physical chemistry properties; (iii) biophysical affinity and activity with bio-macromolecules; (iv) macroscopic physiological effects on human body.

MoleculeNet contributes a data-loading framework, featurization methods, data splitting methods, and learning models to the open source DeepChem package (Figure 1). By adding interchangeable featurizations, splits and learning models into the DeepChem framework, we can apply these primitives to the wide range of datasets in MoleculeNet.

Broadly, our results show that graph convolutional models outperform other methods by comfortable margins on most datasets, revealing a clear advantage of learnable featurizations. However, this effect only holds true when all methods have similar featurizations. For the PDBBind and QM7/7b datasets, the use of featurization which contains pertinent information is more significant than choice of model. Within the domain of models encompassing fully connected neural networks, random forests, logistic regression, and other comparatively simple algorithms, we claim that the PDBbind and QM7/7b results emphasize the necessity of using specialized features for different tasks. While out of the scope of this paper, we note that customized deep learning algorithms<sup>58</sup> could in principle supplant the need for hand-derived, specialized features in such biophysical settings. On the FreeSolve dataset, comparison between conventional *ab-initio* calculations and graph convolutional models for the prediction of solvation energies shows that data-driven methods can outperform physical algorithms with moderate amounts of data. These results suggest that data-driven physical chemistry will become increasingly important as methods mature. Results for physiological datasets are currently weaker than for other datasets, suggesting that better featurizations or more data may be required for data-driven physiology to become broadly useful.

By providing a uniform platform for comparison and evaluation, we hope MoleculeNet will facilitate the development of new methods for both chemistry and machine learning. In future work, we hope to extend MoleculeNet to cover a broader range of molecular properties than considered here. For example, 3D protein structure prediction, or DNA topological

modeling would benefit from the presence of strong benchmarks to encourage algorithmic development. Furthermore, there are a number of interesting molecular machine learning methods not benchmarked here<sup>12,59,60</sup> due to difficulty of implementation. We hope that the open-source design of MoleculeNet will encourage researchers to contribute implementations of these and other algorithms to the benchmark suite. In time, we hope to see MoleculeNet grow into a comprehensive resource for the molecular machine learning community.

## Acknowledgement

We would like to thank the Stanford Computing Resources for providing us with access to the Sherlock and Xstream GPU nodes. Thanks to Steven Kearnes and Patrick Riley for early discussions about the MoleculeNet concept. Thanks to Aarthi Ramsundar for help with diagram construction.

B.R. was supported by the Fannie and John Hertz Foundation.

## Appendix

### Model Training

All models were trained on Stanford’s GPU clusters via DeepChem. No model was allowed to train for more than 10 hours. The total benchmark suite takes about 30 hours to run to completion. Users can reproduce benchmarks locally by following directions from DeepChem.

### Benchmark Reproducibility

Benchmarks were run with numerical seeds fixed, and data splitting methods have been set to maintain deterministic behavior. These settings control most randomness in learning process, but benchmark runs may vary on the order of 1% due to other sources of nondeterminism between runs.



## Model Hyperparameters

### Random Forest

- number of trees in the forest: 500

other settings use the default of Scikit-Learn's Random Forest Classifier/Regressor.<sup>20</sup>

### Logistic Regression

- Optimizer: Adam optimizer with learning rate 0.005
- L2 regularization: 0.1
- Minibatch size: 50
- Number of epochs: 10

### IRV

- K(number of nearest neighbors): 10
- Optimizer: Adam optimizer with learning rate 0.001
- Minibatch size: 50
- Number of epochs: 10

### Multitask Networks(classification)

- Layer structure: one layer with 1500 nodes
- Optimizer: Adam optimizer with learning rate 0.001
- L2 regularization: 0.1
- Dropout: 0.5

- Minibatch size: 50
- Number of epochs: 10

### **Multitask Networks(regression)**

- Layer structure: two layers, both with 1000 nodes
- Optimizer: Adam optimizer with learning rate 0.0008
- L2 regularization: 0.0005
- Dropout: 0.25
- Minibatch size: 128
- Number of epochs: 50

### **Bypass Networks**

- Main layer structure: one layer with 1500 nodes
- Bypass layer structure: one layer with 200 nodes for each task
- Optimizer: Adam optimizer with learning rate 0.0005
- L2 regularization: 0.1
- Dropout: 0.5 for both main and bypass layers
- Minibatch size: 50
- Number of epochs: 10

## Graph Convolutions

- Layer structure: two blocks of graph convolution, each with 64 filters; followed by one fully connected layer with 128 nodes
- Optimizer: Adam optimizer with learning rate 0.0005
- Minibatch size: 50
- Number of epochs: 15

## References

- (1) LeCun, Y.; Bengio, Y.; Hinton, G. *Nature* **2015**, *521*, 436–444.
- (2) Ma, J.; Sheridan, R. P.; Liaw, A.; Dahl, G. E.; Svetnik, V. *Journal of chemical information and modeling* **2015**, *55*, 263–274.
- (3) Ramsundar, B.; Kearnes, S.; Riley, P.; Webster, D.; Konerding, D.; Pande, V. *arXiv preprint arXiv:1502.02072* **2015**,
- (4) Unterthiner, T.; Mayr, A.; Unter Klambauer, G.; Steijaert, M.; Wenger, J.; Ceulemans, H.; Hochreiter, S. Deep Learning as an Opportunity in Virtual Screening. Deep Learning and Representation Learning Workshop (NIPS 2014). 2014.
- (5) Wallach, I.; Dzamba, M.; Heifets, A. *arXiv preprint arXiv:1510.02855* **2015**,
- (6) Delaney, J. S. *Journal of Chemical Information and Modeling* **2004**, *44*, 1000–1005.
- (7) Rupp, M.; Tkatchenko, A.; Müller, K.-R.; Lilienfeld, O. A. v. *Physical Review Letters* **2012**, *108*, 058301.
- (8) Montavon, G.; Rupp, M.; Gobre, V.; Vazquez-Mayagoitia, A.; Hansen, K.; Tkatchenko, A.; Müller, K.-R.; Lilienfeld, O. A. v. *New Journal of Physics* **2013**, *15*, 095003.

- (9) Mobley, D. L.; Guthrie, J. P. *Journal of Computer-Aided Molecular Design* **2014**, *28*, 711–720.
- (10) Rogers, D.; Hahn, M. *Journal of Chemical Information and Modeling* **2010**, *50*, 742–754.
- (11) Duvenaud, D.; Maclaurin, D.; Aguilera-Iparraguirre, J.; Gómez-Bombarelli, R.; Hirzel, T.; Aspuru-Guzik, A.; Adams, R. P. *arXiv preprint arXiv:1509.09292* **2015**,
- (12) kearnes, s.; McCloskey, K.; Berndl, M.; Pande, V.; Riley, P. *arXiv preprint arXiv:1603.00856* **2016**,
- (13) Miller, G. A. *Communications of the ACM* **1995**, *38*, 39–41.
- (14) Deng, J.; Dong, W.; Socher, R.; Li, L.-J.; Li, K.; Fei-Fei, L. ImageNet: A Large-Scale Hierarchical Image Database. CVPR09. 2009.
- (15) Russakovsky, O.; Deng, J.; Su, H.; Krause, J.; Satheesh, S.; Ma, S.; Huang, Z.; Karpathy, A.; Khosla, A.; Bernstein, M.; Berg, A. C.; Fei-Fei, L. *International Journal of Computer Vision (IJCV)* **2015**, *115*, 211–252.
- (16) Krizhevsky, A.; Sutskever, I.; Hinton, G. E. ImageNet Classification with Deep Convolutional Neural Networks. NIPS Proceedings. 2012.
- (17) Szegedy, C.; Liu, W.; Jia, Y.; Sermanet, P.; Reed, S.; Anguelov, D.; Erhan, D.; Vanhoucke, V.; Rabinovich, A. *arXiv preprint arXiv:1409.4842* **2014**,
- (18) He, K.; Zhang, X.; Ren, S.; Sun, J. *arXiv preprint arXiv:1512.03385* **2015**,
- (19) DeepChem: Deep-learning models for Drug Discovery and Quantum Chemistry. <https://github.com/deepchem/deepchem>, Accessed: 2016-12-10.
- (20) others,, et al. *Journal of Machine Learning Research* **2011**, *12*, 2825–2830.
- (21) others,, et al. *arXiv preprint arXiv:1603.04467* **2016**,

- (22) Sheridan, R. P. *Journal of chemical information and modeling* **2013**, *53*, 783–790.
- (23) Bolton, E. E.; Wang, Y.; Thiessen, P. A.; Bryant, S. H. *Annual reports in computational chemistry* **2008**, *4*, 217–241.
- (24) Wang, T.; Xiao, J.; Suzek, T. O.; Zhang, J.; Wang, J.; Zhou, Z.; Han, L.; Karapetyan, K.; Dracheva, S.; Shoemaker, B. A.; Bolton, E.; Gindulyte, A.; Bryant, S. H. *Nucleic Acids Research* **2012**, *40*, D400–D412.
- (25) Gražulis, S.; Chateigner, D.; Downs, R. T.; Yokochi, A.; Quirós, M.; Lutterotti, L.; Manakova, E.; Butkus, J.; Moeck, P.; Le Bail, A. *Journal of Applied Crystallography* **2009**, *42*, 726–729.
- (26) Groom, C. R.; Bruno, I. J.; Lightfoot, M. P.; Ward, S. C. *Acta Crystallographica Section B: Structural Science, Crystal Engineering and Materials* **2016**, *72*, 171–179.
- (27) Berman, H.; Henrick, K.; Nakamura, H. *Nature Structural & Molecular Biology* **2003**, *10*, 980–980.
- (28) Quantum Machine. <http://quantum-machine.org/datasets/>.
- (29) Weininger, D. *Journal of chemical information and computer sciences* **1988**, *28*, 31–36.
- (30) Blum, L. C.; Reymond, J.-L. *Journal of the American Chemical Society* **2009**, *131*, 8732–8733.
- (31) Mobley, D. L.; Wymer, K. L.; Lim, N. M.; Guthrie, J. P. *Journal of Computer-Aided Molecular Design* **2014**, *28*, 135–150.
- (32) Rohrer, S. G.; Baumann, K. *Journal of Chemical Information and Modeling* **2009**, *49*, 169–184.
- (33) Wang, R.; Fang, X.; Lu, Y.; Wang, S. *Journal of Medicinal Chemistry* **2004**, *47*, 2977–2980.

- (34) Wang, R.; Fang, X.; Lu, Y.; Yang, C.-Y.; Wang, S. *Journal of Medicinal Chemistry* **2005**, *48*, 4111–4119.
- (35) Liu, Z.; Li, Y.; Han, L.; Li, J.; Liu, J.; Zhao, Z.; Nie, W.; Liu, Y.; Wang, R. *Bioinformatics* **2014**, *31*, 405–412.
- (36) AIDS Antiviral Screen Data. <https://wiki.nci.nih.gov/display/NCIDTPdata/AIDS+Antiviral+Screen+Data>, Accessed: 2017-02-23.
- (37) Tox21 Challenge. <https://tripod.nih.gov/tox21/challenge/>, Accessed: 2017-02-11.
- (38) Richard, A. M. et al. *Chemical Research in Toxicology* **2016**, *29*, 1225–1251.
- (39) Kuhn, M.; Letunic, I.; Jensen, L. J.; Bork, P. *Nucleic Acids Research* **2016**, *44*, D1075–D41079.
- (40) Altae-Tran, H.; Ramsundar, B.; Pappu, A. S.; Pande, V. *arXiv preprint arXiv:1611.03199* **2016**,
- (41) Medical Dictionary for Regulatory Activities. <http://www.meddra.org/>, Accessed: 2016-09-20.
- (42) Altae-Tran, H.; Ramsundar, B.; Pappu, A. S.; Pande, V. *arXiv preprint arXiv:1611.03199* **2016**,
- (43) Gayvert, K. M.; Madhukar, N. S.; Elemento, O. *Cell Chemical Biology* **2016**, *23*, 1294–1301.
- (44) Artemov, A. V.; Putin, E.; Vanhaelen, Q.; Aliper, A.; Ivan, V. **2016**, 1–20.
- (45) Bemis, G. W.; Murcko, M. A. *Journal of Medicinal Chemistry* **1996**, *39*, 2887–2893.
- (46) Landrum, G. RDKit: Open-Source Cheminformatics Software. <https://www.rdkit.org/>.

- (47) Jain, A. N.; Nicholls, A. *Journal of Computer-Aided Molecular Design* **2008**, *22*, 133–139.
- (48) *The Elements of Statistical Learning: Data Mining, Inference, and Prediction*.
- (49) Gómez-Bombarelli, R.; Duvenaud, D.; Hernández-Lobato, J. M.; Aguilera-Iparraguirre, J.; Hirzel, T. D.; Adams, R. P.; Aspuru-Guzik, A. *arXiv preprint arXiv:1610.02415* **2016**,
- (50) Durrant, J. D.; McCammon, J. A. *Journal of Chemical Information and Modeling* **2011**, *51*, 2897–2903.
- (51) Da, C.; Kireev, D. *Journal of chemical information and modeling* **2014**, *54*, 2555–2561.
- (52) Ramsundar, B.; Liu, B.; Wu, Z.; Verras, A.; Tudor, M.; Sheridan, R. P.; Pande, V. *In Preparation*
- (53) Swamidass, S. J.; Azencott, C.-A.; Lin, T.-W.; Gramajo, H.; Tsai, S.-C.; Baldi, P. *Journal of chemical information and modeling* **2009**, *49*, 756–766.
- (54) others,, et al. *The annals of statistics* **2000**, *28*, 337–407.
- (55) Breiman, L. *Machine learning* **2001**, *45*, 5–32.
- (56) Kearnes, S.; Goldman, B.; Pande, V. *arXiv preprint arXiv:1606.08793* **2016**,
- (57) Ramsundar, B.; Liu, B.; Wu, Z.; Verras, A.; Tudor, M.; Sheridan, R. P.; Pande, V. *Manuscript in preparation*
- (58) Wallach, I.; Dzamba, M.; Heifets, A. *arXiv preprint arXiv:1510.02855* **2015**,
- (59) Lusci, A.; Pollastri, G.; Baldi, P. *Journal of chemical information and modeling* **2013**, *53*, 1563–1575.
- (60) Schütt, K. T.; Arbabzadah, F.; Chmiela, S.; Müller, K. R.; Tkatchenko, A. *arXiv preprint arXiv:1609.08259* **2016**,